Paper:

Dynamic Response of Tall Buildings on Sedimentary Basin to Long-Period Seismic Ground Motion

Nobuo Fukuwa, Takashi Hirai†, Jun Tobita, and Kazumi Kurata

Nagoya University
Furo-cho, Chikusa-ku, Nagoya 464-8601, Japan
†Corresponding author, E-mail: hirai@nagoya-u.jp
[Received February 29, 2016; accepted September 2, 2016]

Characteristics of long-period seismic ground motion and response of tall buildings are investigated in this paper to promote earthquake proof countermeasures considering the damage caused by the 2011 Tohoku earthquake. 3D finite difference method and the reciprocal theorem are used to examine the effect of sedimentary basin structures on seismic wave amplification. Natural period and damping of tall buildings are evaluated by ambient vibration tests and earthquake response observation during construction or demolition of the buildings. The effects of dynamic soil-structure interaction on response amplification of tall buildings are confirmed applying wave propagation theory to a continuum building model. Finally, a newly built base-isolated building with an isolated rooftop laboratory is introduced for full-scale long-period shaking experiment by installing actuators and jacks. Experience of long-period shaking in the building is also available with virtual reality view of indoor damage, which is effective for promotion of seismic countermeasures such as fixing furniture and safe evacuation.

Keywords: long-period long-term ground motion, natural period, damping, vibration experiment, virtual reality

1. Introduction

In the 2011 Tohoku earthquake, high-rise buildings in the metropolitan cities of Tokyo and Osaka shook extensively. In particular, a 256 m tall high-rise building located in the Osaka bay area at a distance of 770 km away from the epicenter shook with a response as large as 137 cm. The input motion at seismic bedrock of Konohana site, near the above building, showed remarkable amplification at the top of the building by a factor of 1,000 at the building's natural period of 6.7 s component [1–3]. A reason for this phenomenon was the sedimentary basin structure in the Osaka plain that increased the ground amplification. Another reason was the similarity of the predominant period of input ground motion to the natural period of the building.

Moreover, at the end of 2015, the Cabinet Office of Japanese Government announced the prediction results of the long-period ground motion caused by the Nankai Trough earthquake [4]. The Ministry of Land, Infrastructure and Transport also proposed measures for tall buildings to protect against long-period ground motions [5]. Such actions reflect the forecast of strong, long-period ground motions in the Osaka and Nobi plains. The advancements in seismic countermeasures are necessary for protecting tall buildings and indoor safety.

In this paper, the characteristics of long-period ground motions in a large-scale sedimentary basin and the response of tall buildings are investigated. Newly developed dynamic experiment devices and shaking experience environment are also introduced for promotion of seismic countermeasures for tall buildings against long-period ground motions.

Based on the ground motion records of the ground surface and the seismic bedrock during the Tohoku earthquake at Konohana site, the amplification of the long-period ground motion cannot be explained by the response amplification of a horizontally layered soil. Moreover, an analysis of the past observation records at the site has confirmed that the predominant period of the ground motion varies [6]. This phenomenon is related to the fact that the sedimentary basin in Osaka plain has topographic subsurface irregularity [7]. Therefore, we used a 3D finite difference method and the reciprocal theorem to examine the effects of the basin structure of Osaka plain on the seismic amplification characteristics [8].

In general, the response amplification in a building is determined by natural period and damping characteristics [9]. However, there is a limited amount of observation data on various kind of buildings [10] and the dynamic characteristics are also affected by the soil-structure interaction. Hence, this study aimed to understand the dependence of dynamic characteristics on the number of floors of a building by introducing a new microtremor and earthquake response observation procedure in tall buildings during construction and demolition. We also demonstrated the effects of dynamic soil-structure interaction on the amplification response based on the wave theory by modeling the building as a continuum.

Finally, we built a system for a full-scale excitation experiment by using a newly built base-isolated building with an isolated rooftop laboratory. Actuators and jacks are equipped for shaking the rooftop isolated mass and

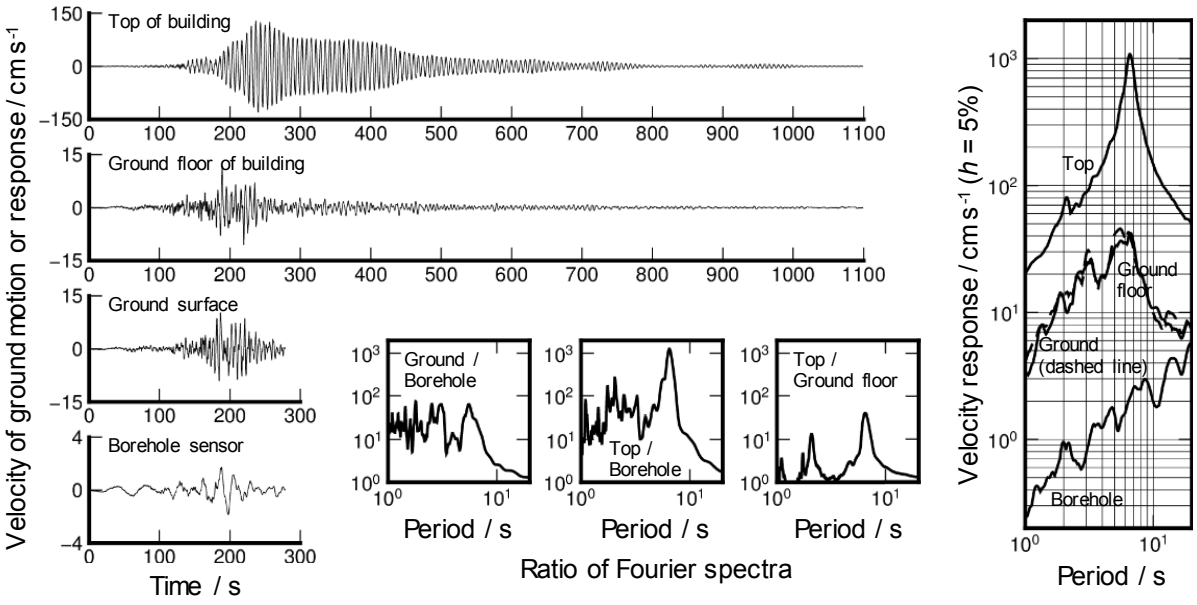

Fig. 1. Velocity waveforms, Fourier spectral ratios, and velocity response spectra recorded at a 256 m tall building and at a neighboring ground (Konohana site) during 2011 Tohoku earthquake.

building itself. We used this system to develop a virtual reality environment to promote seismic countermeasures for buildings and indoor safety such as fixing furniture.

2. Amplification and Elongation of Ground Motion in Sedimentary Basin

Figure 1 shows the velocity response on the 52nd and 1st floors of a 256 m tall building located in the Osaka bay area. It also shows the velocity waveforms recorded at Konohana site in the EW direction on the ground surface and 1600 m below the surface, and their Fourier spectral ratios and velocity response spectra during the Tohoku earthquake.

The figure shows the large amplification at the period of 6–7 s. The resonant amplitude on the 52nd floor is approximately 1000 times as high as that of the bedrock. Since the predominant period of the seismic ground motion and the natural period of the building are similar, the amplification of the response is due to resonance.

According to the information opened on the Web site of KiK-net, the soil structure at Konohana site consists of three layers. The top layer has the thickness of 600 m and the S wave velocity of 500 m/s. The second layer has the thickness of 1000 m and the S wave velocity of 900 m/s. Beneath all the layers, there is the seismic bedrock with the S wave velocity of 3000 m/s. Assuming a horizontally layered soil, the predominant period for a vertically incident S wave is 7.4 s, and the amplification factor is 20. However, the value of the amplification factor is lower than the value observed during the Tohoku earthquake. Fourier spectra of seismic ground motions for four earthquakes observed at Konohana site are compared in **Fig. 2**. They show variation in the predominant period.

The response amplification in the sedimentary basin and the variation in the predominant period could be due to the irregularity in the sedimentary basin structure of the Osaka plain. The Osaka sedimentary basin has almost the elliptical shape, which major and minor axes are about 80 km and 40 km, respectively. The Konohana site is located at slightly the northeast of the center of the sedimentary basin. Therefore, we use a 3D finite difference method and the reciprocal theorem of Green's function [8] to examine the effects of the sedimentary basin structure of the Osaka plain on the amplification characteristics of the ground motion.

Here we define Green's function as the relationship between the moment tensor at the source and the displacement vector at the station. The 3D finite difference method is employed to calculate Green's function referring the reciprocity of Green's function. In general, the 3D finite difference method is effective for estimating the ground motion in whole region of the model for a certain earthquake. It is therefore suitable for predicting the ground motions at multiple points for one seismic source. On the other hand, the method used in this paper is effective for predicting the ground motion at a particular site for multiple sources. It allows us to efficiently examine the effect of the source location and the sedimentary basin structure in the Osaka plain on the characteristics of soil amplification.

In this study, the soil structure model previously used at the headquarters of the earthquake research promotion is used to predict the long-period ground motions. **Fig. 3** shows the distribution of the depth of the seismic bedrock. The observation site is at the surface of Konohana site. Point sources with the strike angle of 22.5° from the radial axis, the dip angle of 90°, the rake angle of 0°, and the moment magnitude of 7.0 are assumed. The epicentral

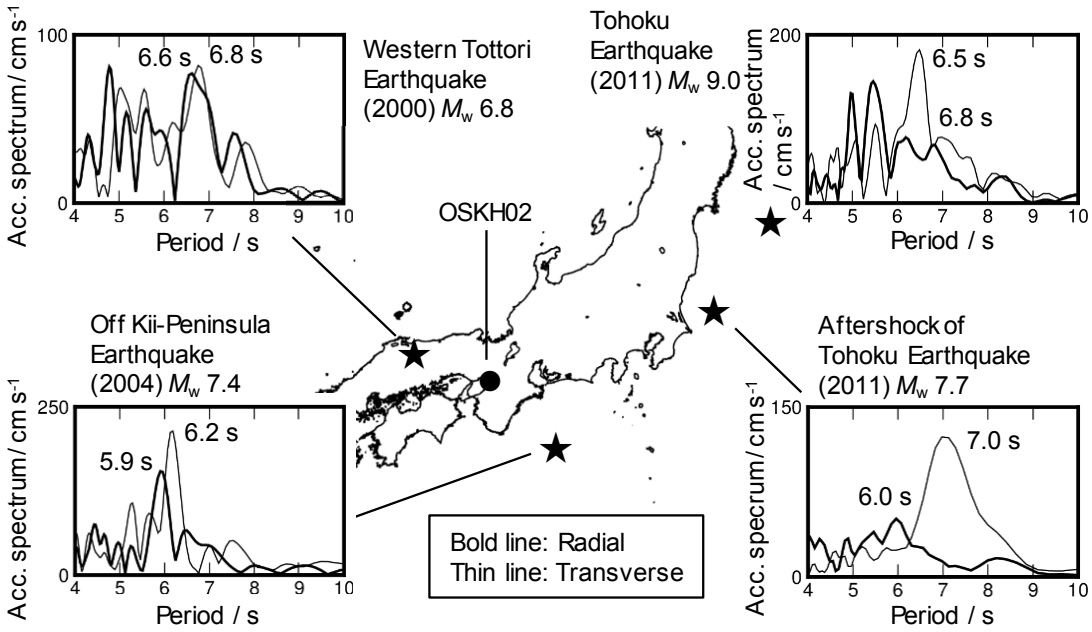

Fig. 2. Fourier spectra of the ground accelerations recorded at Konohana site.

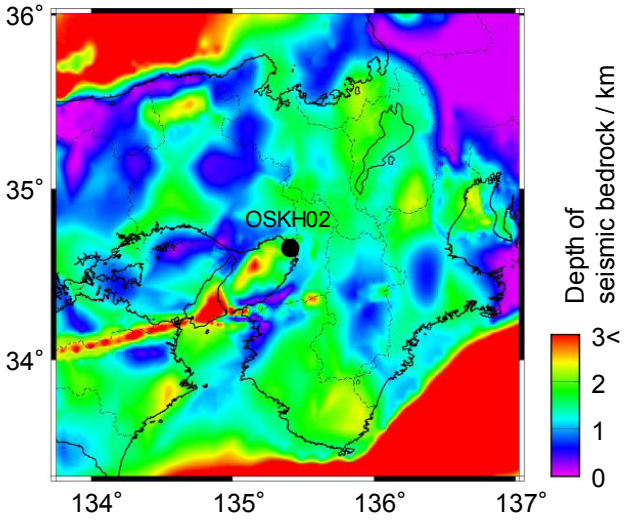

Fig. 3. Distribution of the depth of the seismic bedrock in the analysis region.

distance R is assumed the two cases of 50 km and 100 km. Similarly, the focal depth D is assumed the two cases of 10 km and 100 km.

The finite difference analysis is based on Graves's staggered-grid method [11] and Levandar's fourth-order difference formulation [12]. The grid shape is cubic and its sides are 300 m for the depth of 15 km below the ground surface. The sides of the grids are 900 m beyond 15 km. The boundary between the grids at the depth of 15 km is treated by the method of Aoi and Fujiwara [13]. The period allowed in this analysis is above 3 s. The non-reflecting boundary condition by Clayton and Engquist [14] and the energy-absorbing boundary condition with a thickness of 18 km by Cerjan et al. [15] are applied to the edges of computing regions.

Figure 4 shows the displacement waveforms, particle motions, and velocity response spectra on the surface and in the seismic bedrock for the sources with the same epicentral distances to Konohana site. The origin of the particle motion corresponds to the epicenter. The figure demonstrates that regardless of the same epicentral distances, the amplitude and direction of the particle motion vary and are dependent on the source location. This is due to the shape of the sedimentary basin in the Osaka plain. The variation in the ground motion shown in **Figs. 4(a)** and **(b)** due to the source direction is larger than those in **Figs. 4(c)** and **(d)**. This is because the seismic waves from deeper sources have larger incident angles. This decreases the effects of the irregularity of the shallow soil structure. Moreover, the comparison between **Figs. 4(a)** and **(b)** and **Figs. 4(e)** and **(f)** reveals that both cases have similar variations in the ground motion due to the source direction. The above results indicate that the variation in the seismic ground motion due to the source direction is largely caused by the irregular soil structure near Konohana site.

Figure 5 shows the Fourier spectral ratios on the ground surface and in the seismic bedrock for the sources with same epicentral distances to Konohana site. The red color corresponds to the spectral ratio for the source in the north, and the blue color corresponds to that in the south. The colors are changed continuously depending on the source direction. The spectral ratios do not change continuously with the change in the source direction. They seem to reflect the irregularity of the soil structure of the Osaka sedimentary basin in a complex manner. Additionally, we studied the peaks in the spectral ratios by grouping them into peaks with a period of 5 s and those with a period of approximately 6–7 s. The peaks in the former

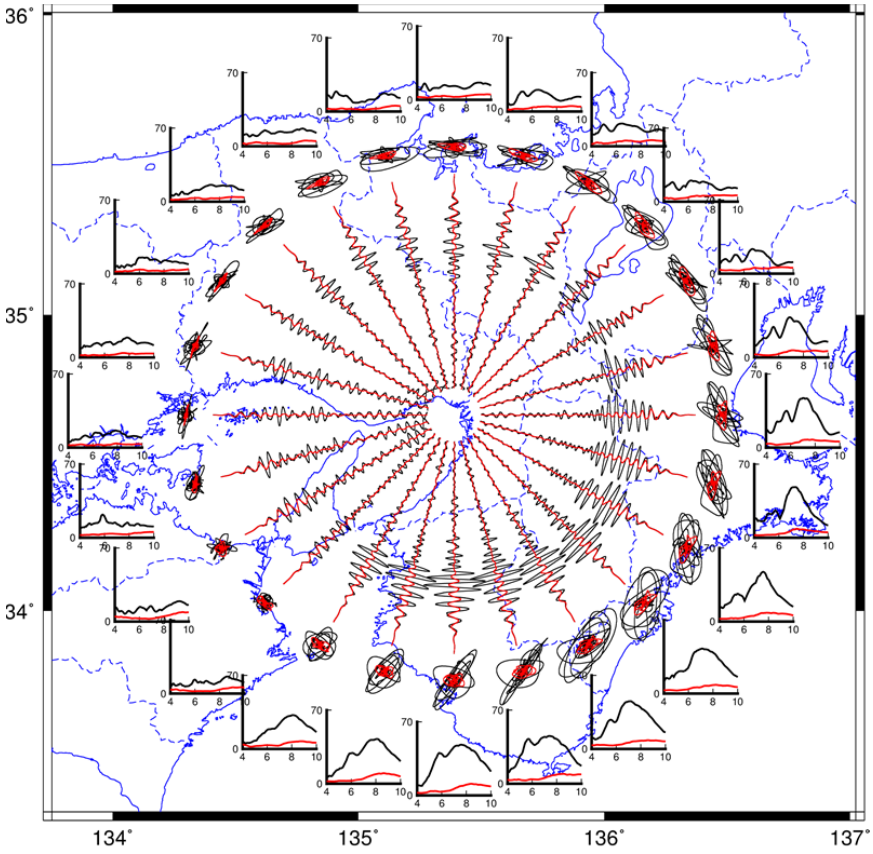

(a) $R = 100$ km, $D = 10$ km, Radial

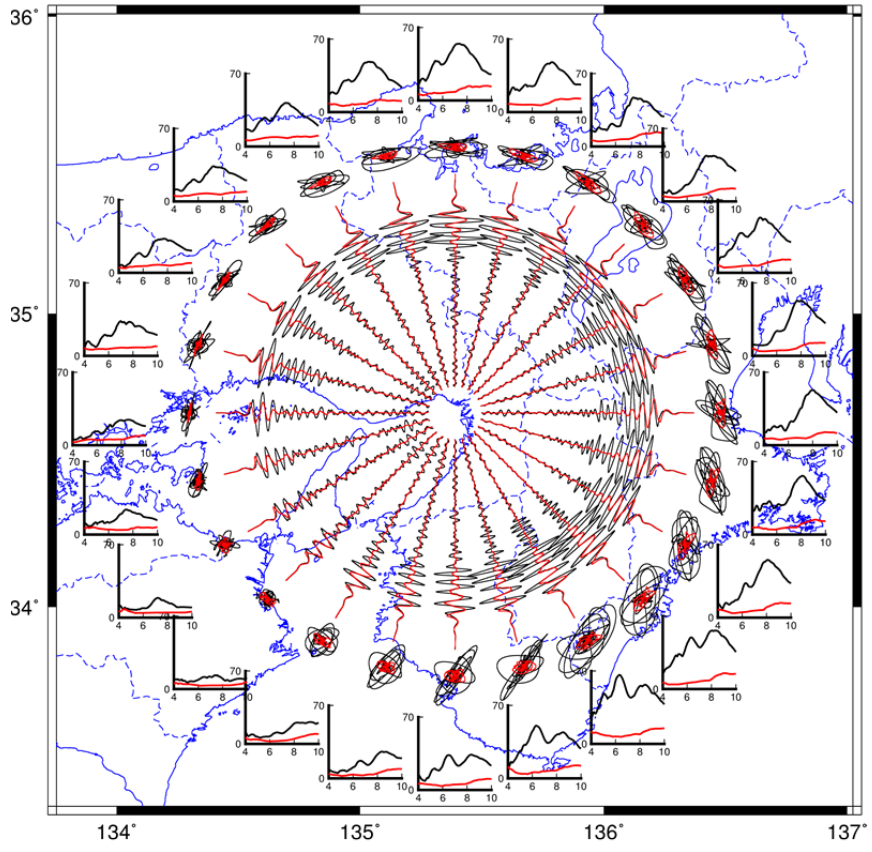

(b) $R = 100$ km, $D = 10$ km, Transverse

Fig. 4. Displacement waveforms, particle motions, and velocity response spectra on the ground surface and in the seismic bedrock. R and D denote the epicentral distance and the focal depth, respectively. Black and red lines correspond to the ground surface and the seismic bedrock, respectively.

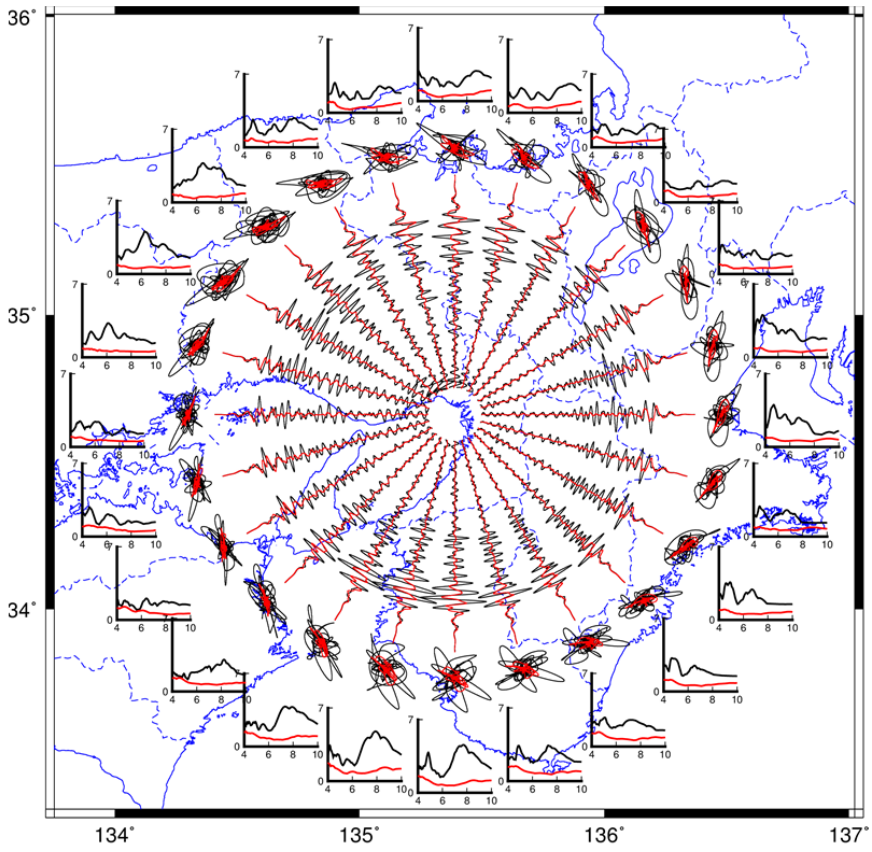

(c) $R = 100$ km, $D = 100$ km, Radial

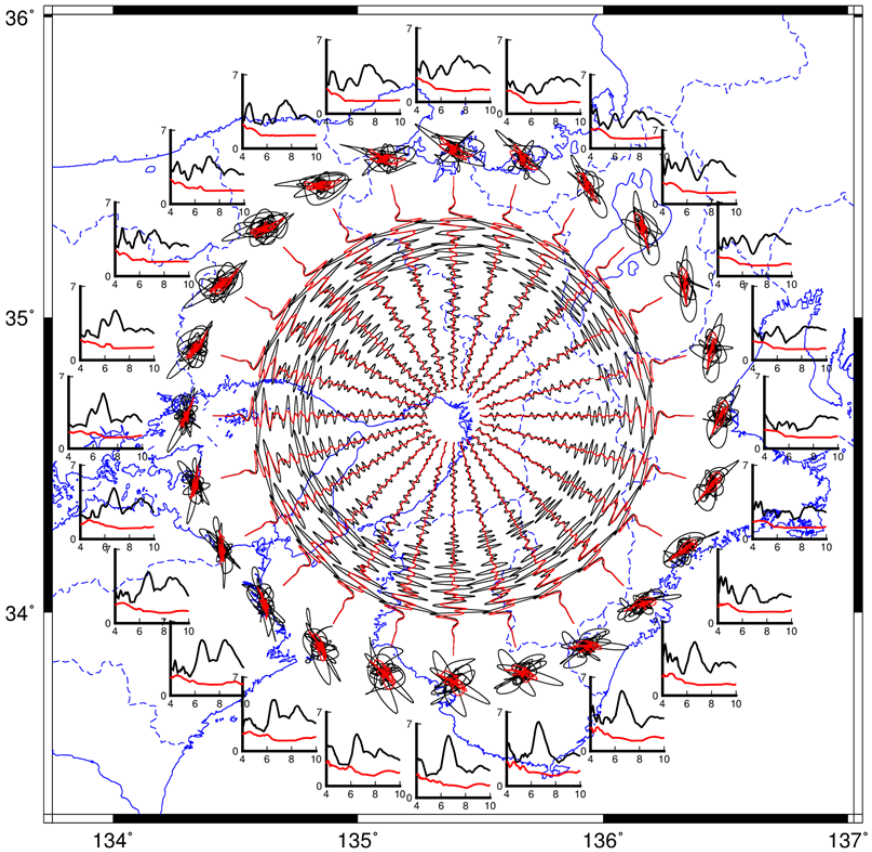

(d) $R = 100$ km, $D = 100$ km, Transverse

Fig. 4. Continued.

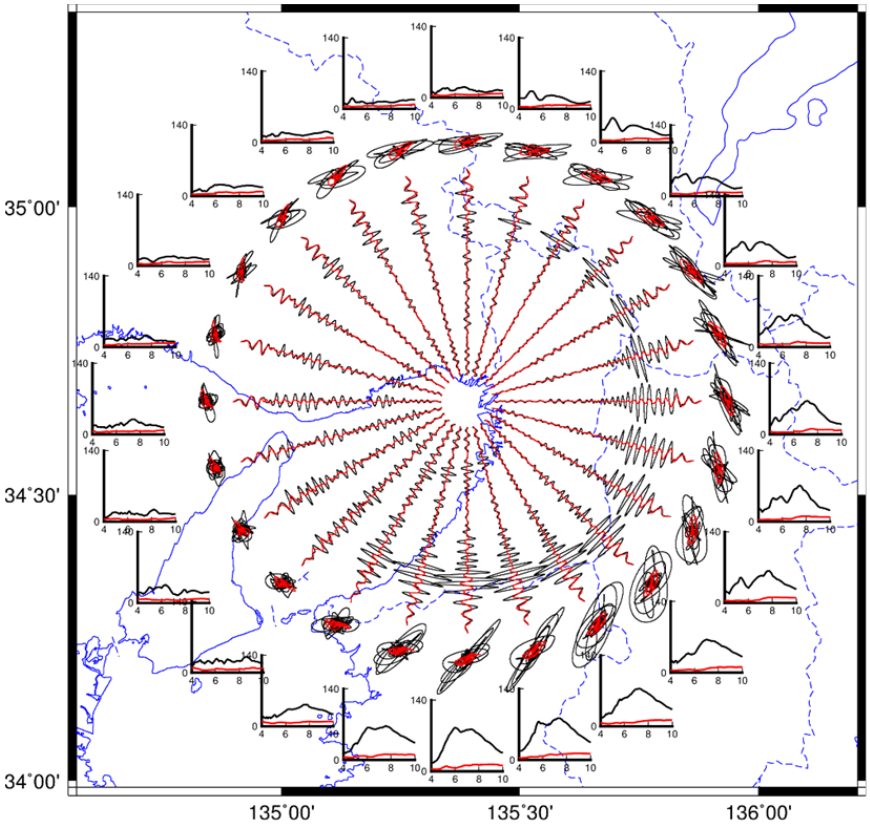

(e) $R = 50$ km, $D = 10$ km, Radial

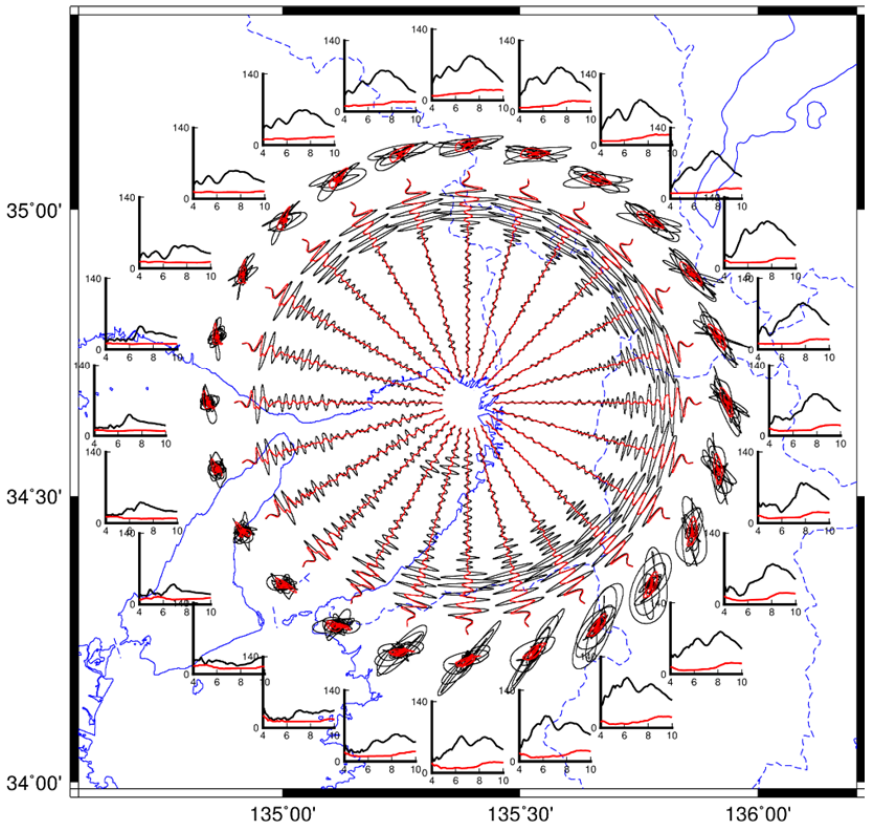

(f) $R = 50$ km, $D = 10$ km, Transverse

Fig. 4. Continued.

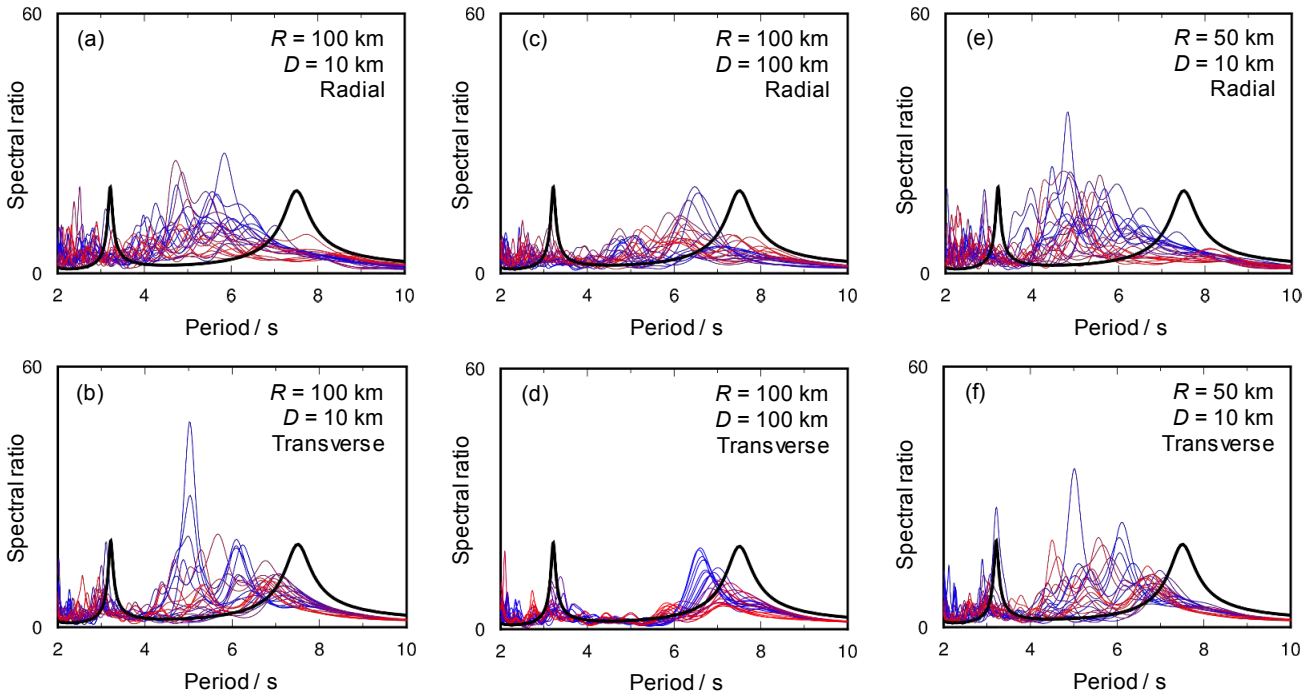

Fig. 5. Fourier spectral ratios between the ground surface and in the seismic bedrock. R and D denote the epicentral distance and the focal depth, respectively. Red color corresponds to the seismic source in the north, while blue color corresponds to that in the south. Black lines denote the Fourier spectral ratios for the layered soil structure.

group appear in **Figs. 5(a)**, **(b)**, **(e)** and **(f)** (focal depth of 10 km) in both the radial and transverse components but do not exist in **Figs. 5(c)** and **(d)** (focal depth of 100 km). Conversely, the peaks in the latter group are prominent in **Figs. 5(c)** and **(d)** but not in **Figs. 5(a)**, **(b)**, **(c)**, and **(d)**. In general, surface waves are dominant for shallow seismic sources, and body waves are dominant for deep seismic sources. Therefore, it is suggested that the peaks with periods of approximately 5 s corresponds to the amplification of the surface waves, while those with periods of approximately 6–7 s corresponds to the vertically incident body waves. It sould be noted that the predicted peaks of the Fourier spectral ratios for the used soil model (colored lines) are less than those for the horizontally layered soil (black lines).

In conclusion of this section, it was revealed that the property of the seismic ground motion varies with respect to the source direction and the focal depth. Such an effect cannot be explained under the assumption of the parallel layered soil structure, but the trend of the ground motion variation can be estimated using the method described in this section.

3. Response Characteristics of Tall Buildings

The response characteristics of a building are expressed by the natural period and the modal damping factor of the building. It is generally believed that the fundamental natural period linearly increases with the building height, while the modal damping factor is inversely proportional to the height [9–10]. **Fig. 6** shows the summary of the dependence of fundamental natural period and damping factor on the building height. **Fig. 6** includes the data from nine buildings shown in **Table 1** [9, 16–19]. For each building, continuous vibration observations were performed during construction and demolition, and thus, different characteristics for varying heights were measured for a building with the same soil and foundation conditions. This leads getting clear tendency of vibration characteristics for different height of buildings comparing to the most of previous researches.

As in **Table 1**, the upper parts of the high-rise buildings Nos.1–5 are steel structures. The middle-rise buildings Nos.6–9 include S, RC, and PC structures. No.6 is a base-isolated building, but its characteristics appeared similar to others in terms of low-level vibration. This is due to the non-linearity of the seismic isolator.

Figure 6(a) shows a proportional trend of the fundamental natural period with respect to height. A building shows continuous change in its construction or demolition, while there is a variation in the slope arising from the difference of structural system and materials of the building. Steel framed structures show a tendency of longer natural periods, however, reinforced concrete buildings (Nos.6, 8, and 9) and a steel structure with rigid elliptical core (No.3) have shorter natural periods. Such characteristics are examined for various conditions of buildings [10], $T = 0.03H$ with natural period T and building height H is used for steel buildings and $T = 0.02H$ is for reinforced concrete buildings. Comparing to these equations, tendency of natural period in **Fig. 6(a)** is rela-

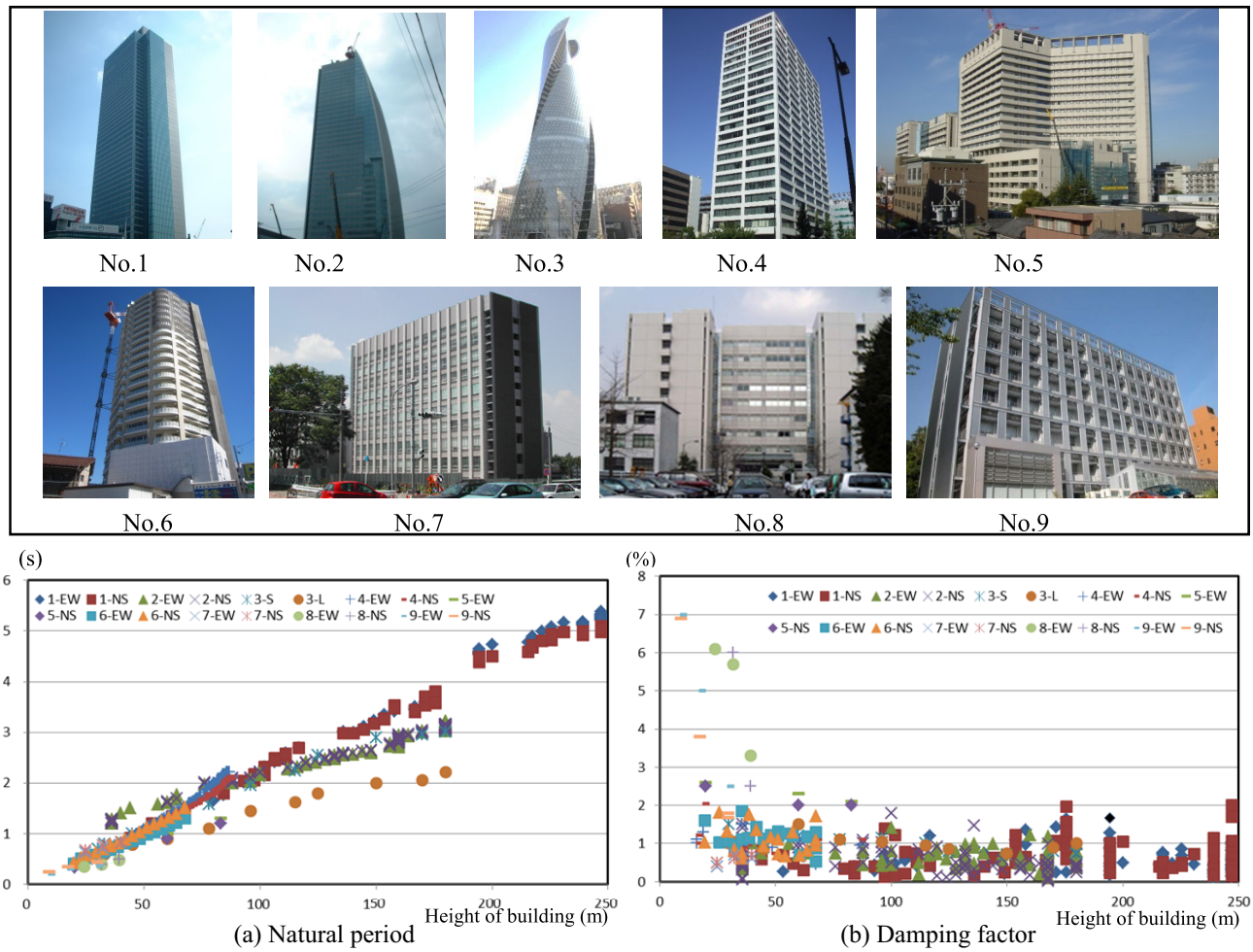

Fig. 6. Natural period and damping for different height buildings including under construction and demolition stages.

Table 1. Outline of observed buildings.

Bldg. No.	Height (m)	Superstructure floors	Basement floors	Typical floor size (m) and shape	Structure	With or without base-isolation and vibration control devices	Built year	Designed horizontal natural period (s)	Observation year
1	247	47	6	51 × 51	Steel, SRC for basement	Damper, Tuned Mass Damper(TMD), Active Tuned Mass Driver(ATMD), building connection damper	2006	EW: 5.75, NS: 5.92	2005–06
2	180	42	3	54 × 52	Steel, SRC for basement	Damper	2006	EW: 4.21, NS: 3.86	2005–06
3	170	36	3	30 × 21 oval shaped core	Steel, SRC for basement	Damper, TMD, AMD	2008	Short: 2.95, long: 2.23	2007–
4	90	25	3	55×30	Steel, SRC for basement	—	1973	EW: 2.47, NS: 2.44	2009–10
5	85	17	2	80 × 61 irregular plan	Steel, SRC for basement	Viscous devices	2003	—	2001–03
6	68	21	0	33.5 × 23.3	RC	Base-isolation	2013	6.3 (Base-isolated period)	2012–13
7	47	10	1	60 × 15	Steel, SRC for basement	—	2001	1.2	2000–
8	42	10	1	55 × 28 L-shaped plan	SRC	—	1995	—	1995–
9	33	7	1	40 × 14	Precast Concrete, SRC for basement	—	2003	—	2003–

tively short. **Fig. 6(b)** shows a variation in the damping factor, but there is a general tendency of the factor to decrease with increasing height. Most high-rise steel structures show damping factors of 1% or lower. This indicates that the remarkable response amplification will be caused by resonance with long-period and long-duration seismic input motions.

Dynamic characteristics shown in **Fig. 6** are examined

by replacing lumped mass system with a one-dimensional shear, continuum model considering a uniform structure with each floor mass m, stiffness k, story height l, and number of floors n. Generally, the relationship between the building's natural period T and its height H is linear, i.e., $T = \theta H$. Conversely, the fundamental natural period of a contentious body of height H that is fixed at the bottom and free at the top can be expressed by using the shear wave velocity V_b and height H, as $T = 4H/V_b$. Therefore, the equivalent shear wave velocity of a continuum is $V_b = 4/\theta$. In a case of the steel structure, θ is approximately 0.03 s/m and then $V_b = 133$ m/s.

If the weight of a building per unit floor area is w, then the mass density of the continuum ρ_b can be expressed as $\rho_b = w/gl$, where g is the gravitational acceleration. By setting the floor height as 4 m and the floor load as 0.8 tf/m^2, the weight per unit volume is $\gamma_b = 0.2$ tf/m^3. This corresponded to a continuum with a weight per unit volume that is 1/10 of the soil and with a shear wave velocity equivalent to that of the soft soil.

Furthermore, dynamic soil spring of a circular rigid foundation with radius r is given by stiffness K and damping coefficient C as follows:

$$K = \frac{8rG_g}{2-\nu} \quad C = \pi r^2 \rho_g V_g \quad \ldots\ldots\ldots \quad (1)$$

Here G_g, ν, ρ_g, and V_g are shear modulus, Poisson's ratio, mass density, and S wave velocity of soil, respectively. We assumed complex damping for the building's internal damping ratio h, which is sufficiently small ($h \ll 1$). The above conditions give the displacement of the structure u as the ratio to the surface ground motion u_g as follows:

$$\frac{u}{u_g} = \frac{\alpha_b \left(1 - i\frac{\beta}{a_0}\right) \cos k_b z}{\alpha_b \left(1 - i\frac{\beta}{a_0}\right) \cos a_b + i \sin a_b} \quad \ldots\ldots \quad (2)$$

Here

$$\alpha_b = \frac{\rho_g V_g}{\rho_b V_b}, \quad \beta = \frac{8}{\pi(2-\nu)}, \quad k_g = \frac{\omega}{V_g}, \quad a_0 = \frac{\omega r}{V_g} = k_g r, \quad a_b = \frac{\omega H}{V_b} = k_b H \quad (3)$$

In resonance ($a_b = \pi/2$), Eq. (2) is:

$$\frac{u|_{a_b=\frac{\pi}{2}}}{u_g} \approx \frac{\alpha_b \left(1 - i\frac{\beta}{\chi}\right)}{\left[1 + \frac{\pi}{2} h \alpha_b \left(1 - i\frac{\beta}{\chi}\right)\right] i} \quad \ldots\ldots \quad (4)$$

χ is the interaction coefficient and shows large value for stiff buildings with low and wide elevation. In the cases with the interaction coefficient χ is infinite and zero:

$$\lim_{\chi\to\infty} \frac{u|_{a_b=\frac{\pi}{2}}}{u_g} = \frac{\alpha_b}{\left(1 + \frac{\pi}{2} h \alpha_b\right) i} \quad \ldots \quad (5)$$

$$\lim_{\chi\to 0} \frac{u|_{a_b=\frac{\pi}{2}}}{u_g} = \frac{2}{\pi h i}$$

In case of small structural damping h, the resonant amplification becomes the wave impedance ratio of soil and structure, α_b, for a flat and low-rise building (large χ), and the resonant amplification ratio is $2/\pi h$ for a thin, high-rise building (small χ). Therefore, the response of a rigid and heavy building is not significantly amplified, while that of a flexible and light building is amplified. Moreover, in a high-rise building, the damping effect of the vibration damper is large.

An example of a building with high interaction coefficient (rigid and flat) with a small impedance ratio α_b (rigid and heavy) is a nuclear reactor building. A high-rise building on an alluvial plain is an example of building with opposite characters. For a steel structure on a sedimentary soil, α_b is around 10, while for a nuclear reactor building on a rock site, α_b is around 1. As the damping factor of a tall building is about 1–2%, the resonant amplification can be estimated. Such characteristics match the results shown in **Fig. 6**.

4. Environment for Experience of Long-Period Building Response

To enhance the seismic countermeasures for structures and indoor areas against long-period seismic ground motions, it is necessary to build a full-scale shaking facility for structural experiments and shaking experiences. The Disaster Mitigation Research Building was built in the campus of Nagoya University in 2014 as a key-facility for advanced research, educational activity and emergency response against natural disasters. **Fig. 7** shows outline of the building and its experimental setup for long-period motion.

The building is four-story reinforced concrete structure of distinguished triangular shape with approximately 3,000 m^2 floor area and 5,600 t weight. The base-isolation system is equipped at basement floor, which consists of 5 natural rubber bearings, 9 cross linear bearings and 8 oil dampers, showing elastic properties. Fundamental natural period of the building is designed as 5.2 s, which is much higher than the site predominant period of 2.6 s. The clearance of base-isolated layer is 90 cm, which is larger than that of averaged base-isolated buildings. A newly developed pull jacks are installed at basement floor to perform free vibration experiments with initial displacement of 150 mm.

The basement floor is also used as a gallery for learning the history of aseismic structures, base-isolation and vibration control systems. The 1st floor has a disaster mitigation gallery for learning through experiences and the

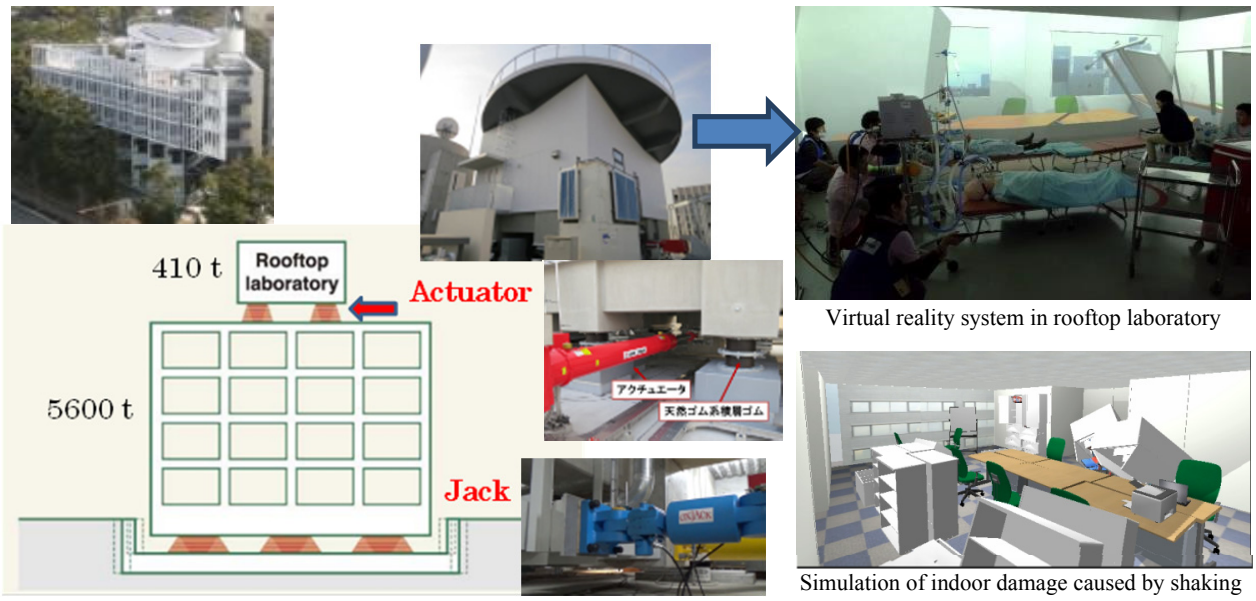

Fig. 7. Vibration experiment environment of the doubly-isolated structure and virtual reality system.

2nd floor has a library. The 3rd and 4th floors are spaces for research projects.

A laboratory room with 410 t weight on the rooftop is also isolated by cross linear bearings and rubber bearings with the same isolation period of 5.2 s. Thus the building is a double base-isolated structure. The rooftop laboratory is able to shake by actuators and the amplitude can be amplified by up to 70 cm when vibrated in resonance by an actuator.

The interior of the laboratory is equipped with visual and audio systems that are synchronized with the vibrations, thereby making up a virtual reality system that can reproduce conditions during earthquakes. The automatic generation of audio is done by a method that uses Causal FFT to reproduce sounds from waveforms [20]. For reproducing the overturning and moving response of furniture, simulation software often used in video games is used [21]. The above facilities make up an environment that allows experiments in psychology during earthquakes and disaster response trainings. For example, a video educational material for the long-period earthquake ground motion is prepared in this facility in collaboration with the Japan Meteorological Agency [22]. **Fig. 8** shows the situation in the laboratory subjected to moderate level of long-period shaking and simulated situation for higher level input.

It is possible to produce an inertial force of 40 t by using the vibration of the roof-top laboratory as the vibration force. This vibrated the main building of 5,600 t by the displacement amplitude of approximately 5 cm. The underground base isolation layer was also equipped with newly developed pull jacks, which enabled free vibration experiments with forced displacements of approximately 15 cm. As shown in **Fig. 7**, the roof-top resonance excitation experiments and the underground free vibration experiments enabled an environment in which we could vibrate a building at will.

The natural periods of the main building and the roof-top laboratory were both 5.2 s. By viewing them as the soil and the building, it was possible to reproduce a resonant response of a tall building. This response was used in the research and development of a vibration control method for avoiding resonance.

Figure 9 shows the displacement response of the roof-top laboratory and the main building during a roof-top laboratory excitation experiment. The figure also demonstrates the displacement response of the main building with and without damper during a free vibration experiment with a forced initial displacement by jacks. The facility is capable of vibrating a building with a mass of 5,600 t. **Fig. 10** illustrates the displacement response of the roof-top laboratory and the main building during free vibration experiment without the underground oil damper. The figure shows the realization of the resonant response experiment for the main building and the base-isolated roof-top laboratory.

In the future, we plan to install an oil damper (which can be switched on and off) on the roof and investigate the effectiveness of TMD for high wind in the presence of the damper. The actuator in the roof-top laboratory also contains a feedback control function. This, in turn, can be used for the development of absolute isolation with AMD.

The building is equipped with a lot of seismometers, earth pressure gauges, and displacement gauges. They can be used for understanding the vibrational behavior of the building, changes in the building and the isolation system over time, and the distribution characteristics of earth pressure during earthquakes. We have placed various simple seismometers and are currently investigating their effectiveness for establishing a cost-effective vibration monitoring method. We plan to develop new vibration monitoring techniques by using these seismometers.

Fig. 8. Photo of the shaking experience laboratory subjected to long-period shaking (top), and simulated situation for higher level shaking (bottom).

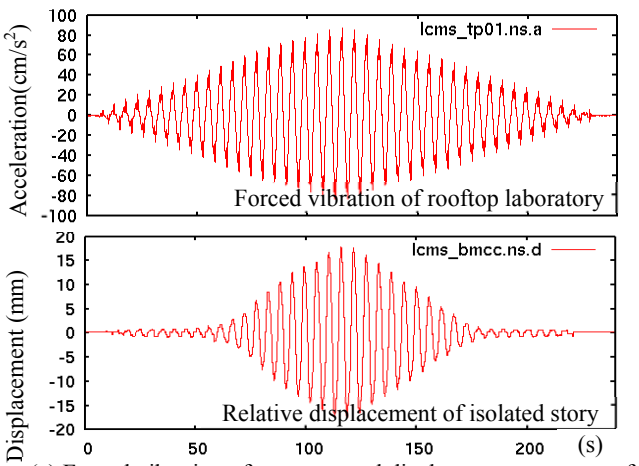

(a) Forced vibration of top mass and displacement response of the isolated building

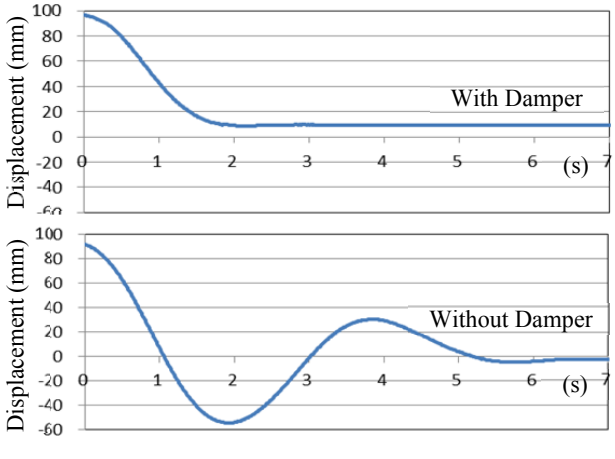

(b) Free vibration of isolated building with initial displacement

Fig. 9. Response of the building under forced vibration and free vibration tests.

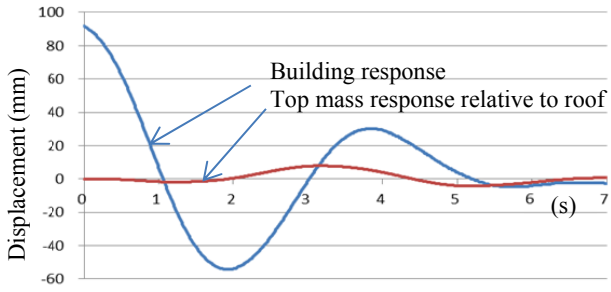

Fig. 10. Relative displacement response of the building and top mass without underground oil damper during free vibration test.

5. Conclusions

This paper elucidated the characteristics of long-period ground motions on a large-scale sedimentary basin and response characteristics of tall buildings through observation records and theoretical calculations. We also realized the Disaster Mitigation Research Building, which could host long-period vibration experiments and allow the experience of long-period motion. We also developed guiding measures for tall buildings against long-period ground motions. The findings can be summarized as follows:

1) The analysis of ground motion records and the theoretical analysis based on the 3D finite difference method and the reciprocal theorem show that the ground motion recorded in the Osaka bay area during the Tohoku earthquake was affected by the sedimentary basin structure of the Osaka plain. The topographic subsurface irregularity of the sedimentary basin caused variation of the predominant period of the ground motion due to the source direction as well as in the response amplification. Therefore, the design of long-period structures must incorporate such variations of the predominant period of the long-period ground motion.

2) Introducing a new observation procedure for a building through whole stages of construction or demolition, we analyzed the dependence of the dynamic characteristics of the buildings on the number of floors. We confirmed that the natural period is proportional to the number of floors and that the damping factor is inversely proportional to the number of floors. We also modeled a structure as a continuum and used the wave propagation theory to investigate the effect of the dynamic soil-structure interaction on the dynamic response characteristics. As a result, we found that resonant response amplification is determined by the wave impedance ratio of the soil to the structure for flat structures and by internal damping for thin and tall structures.

3) We also established that it was possible to use the double base-isolated building to carry out resonance experiments. For example, a resonant vibration experiment could be conducted by resonantly vibrating the roof-top laboratory by an actuator. A free vibration experiment could be conducted in the basement isolation layer by forced displacements produced by jacks. We also realized a virtual reality system that vibrates synchronously with image and sound to experience the response to long-period ground motions. Taken together, the above facilities provided an environment in which advancements can be made in countermeasures for buildings against long-period ground motions.

References:

[1] Osaka General Affairs Department, "Examination results on safety of Sakishima Prefectural Building," May, 2011 (in Japanese).
[2] BRI Strong Motion Observation, http://smo.kenken.go.jp/ja/smreport/201103111446 [accessed July 15, 2016]
[3] NIED Strong-motion Seismograph Networks (K-NET,KiK-net), http://www.kyoshin.bosai.go.jp/ [accessed July 15, 2016]
[4] Cabinet Office, "Examination meeting for modeling great earthquakes in Nankai Trough, examination meeting for modeling earthquakes directly beneath the capital: Report on long-period seismic motions in great earthquakes in Nankai Trough," Dec., 2015 (in Japanese), http://www.bousai.go.jp/jishin/nankai/pdf/jishinnankai20151217_01.pdf [accessed July 15, 2016]
[5] Ministry of Land, Infrastructure and Transport, Housing Bureau, Building Guidance Division, "About countermeasures for super high-rise buildings against long-period seismic motions near Nankai Trough," 2015 (in Japanese).
[6] Y. Terashima, H. Takahashi, N. Fukuwa, and M. Mori, "Study of resonance between high-rise buildings on sedimentary plain and Long-period Ground Motions Part.1 Analysis of ground motion characteristics and strong motion prediction in Osaka basin," Annual Meeting of AIJ, pp. 151-152, 2012 (in Japanese).
[7] Y. Terashima, T. Hirai, and N. Fukuwa, "The effect of sedimentary basin structure on predominant period of seismic ground motion – the analysis using 3-D finite difference method – ," J. of Structural and Construction Engineering , AIJ, Vol.80, No.708, pp. 219-229, 2015 (in Japanese).
[8] T. Hirai and N. Fukuwa, "Evaluation method of dynamic characteristics of sedimentary basin using 3-D finite difference method and reciprocity theorem," J. of Structural and Construction Engineering , AIJ, Vol.78, No.694, pp. 2083-2091, 2015 (in Japanese).
[9] N. Fukuwa and J. Tobita, "Key Parameters Governing the Dynamic Response of Long-Period Structures," J. of Seismology, Vol.12, No.2, pp. 295-306, 2008.
[10] AIJ, "Damping in buildings," Maruzen, 2000 (in Japanese).
[11] R. W. Graves, "Simulating Seismic Wave Propagation in 3D Elastic Media Using Staggered-Grid Finite Differences," Bull. Seism. Soc. Am., Vol.86, pp. 1091-1106, 1996.
[12] A. R. Levander, "Fourth-order Finite Difference P-SV Seismograms," Geophysics, Vol.53, pp. 1425-1436, 1988.
[13] S. Aoi and H. Fujiwara, "3D Finite-Difference Method Using Discontinuous Grids," Bull. Seism. Soc. Am., Vol.89, pp. 918-930, 1999.
[14] R. Clayton and B. Engquist, "Absorbing Boundary Conditions for Acoustic and Elastic Wave Equations," Bull. Seism. Soc. Am., Vol.67, pp. 1529-1540, 1977.
[15] C. Cerjan, D. Kosloff, R. Kosloff, and M. Reshef, "A Non-Reflecting Boundary Condition for Discrete Acoustic and Elastic Wave-Equations," Geophysics, Vol.50, pp. 705-708, 1985.
[16] T. Mastushita, T. Nishizawa, J. Tobita, and N. Fukuwa, "Variation of Vibration Characteristics of a High-rise Building based on Microtremor Observation and Vibration Experiments and Earthquake Response Observation," AIJ J. Technol. Des., Vol.20, No.46, pp. 879-884, 2014 (in Japanese).
[17] J. Tobita, N. Fukuwa, T. Nishizawa, and K. Imaeda, "Long-term Structural Monitoring and Damage Detection of High-rise Buildings by use of Fiber Optic Sensors," Proc. 15th WCEE, Lisbon, 2012.
[18] T. Amano, T. Takahashi, N. Fukuwa, M. Mori, and J. Tobita, "Change of dynamic characteristics of a base-isolated high-rise building based on successive vibration observation during construction," J. Struct. Constr. Eng., AIJ, Vol.79, No.700, pp. 721-730, 2014 (in Japanese).

[19] H. Kojima, N. Fukuwa, and J. Tobita, "Effects of Soil-Structure Interaction Dependent on Number of Stories based on Microtremor and Earthquake Response Observations," J. of Structural Engineering, Vol.48B, pp. 453-460, 2002 (in Japanese).
[20] T. Hirai and N. Fukuwa, "Synthesis of Earthquake Sound Using Seismic Ground Motion Records," Bulletin of the Seismological Society of America, Vol.104, No.4, pp. 1777-1784, 2014.
[21] T. Matsushita, K. Kurata, J. Tobita, N. Fukuwa, M. Yoshizawa, and T. Nagae, "Development of Monitoring System and Simulation of Indoor Situation during Earthquake Based on Shaking Table Experiment," AIJ J. of Technology and Design, Vol.19, No.43, pp. 871-874, 2013 (in Japanese).
[22] Japan Meteorological Agency, "Video for Long-Period Earthquake Motion" (in Japanese), http://www.data.jma.go.jp/svd/eqev/data/choshuki/choshuki_eq5.html [accessed July 15, 2016]

Name:
Nobuo Fukuwa

Affiliation:
Professor, Disaster Mitigation Research Center, Nagoya University

Address:
Furo-cho, Chikusa-ku, Nagoya 464-8601, Japan

Brief Career:
1991- Associate Professor, School of Engineering, Nagoya University
1997- Professor, C. for Cooperative Research in Advanced Science and Technology, Nagoya University
2001- Professor, Graduate School of Environmental Studies, Nagoya University
2012- Professor, Disaster Mitigation Research Center, Nagoya University

Selected Publications:
• "Key Parameters Governing the Dynamic Response of Long-Period Structures," J. of Seismology, Vol.12, No.2, pp. 295-306, 2008.

Academic Societies & Scientific Organizations:
• Architectural Institute of Japan (AIJ)
• Japan Association for Earthquake Engineering (JAEE)

Name:
Takashi Hirai

Affiliation:
Assistant Professor, Graduate School of Environmental Studies, Nagoya University

Address:
Furo-cho, Chikusa-ku, Nagoya 464-8601, Japan

Brief Career:
2013- Assistant Professor, Graduate School of Environmental Studies, Nagoya University

Selected Publications:
• "Evaluation method of dynamic characteristics of sedimentary basin using 3-D finite difference method and reciprocity theorem," J. of Structural and Construction Engineering, AIJ, Vol.78, No.694, pp. 2083-2091, 2015 (in Japanese).

Academic Societies & Scientific Organizations:
• Architectural Institute of Japan (AIJ)
• Japan Association for Earthquake Engineering (JAEE)

Name:
Jun Tobita

Affiliation:
Professor, Disaster Management Office, Nagoya University

Address:
Furo-cho, Chikusa-ku, Nagoya 464-8601, Japan

Brief Career:
1989- Research Associate, Tohoku University
1996- Associate Professor, Nagoya University
2011- Professor, Nagoya University

Selected Publications:
• "Integrated Disaster Simulator using WebGIS and its Application to Community Disaster Mitigation Activities," J. of Natural Disaster Science, Vol.30, No.2, pp. 71-82, 2009.

Academic Societies & Scientific Organizations:
• Architectural Institute of Japan (AIJ)

Name:
Kazumi Kurata

Affiliation:
Assistant Professor, Disaster Mitigation Research Center, Nagoya University

Address:
Furo-cho, Chikusa-ku, Nagoya 464-8601, Japan

Brief Career:
2006- Falcon Corp.
2012- Assistant Professor, Disaster Mitigation Research Center, Nagoya University

Selected Publications:
• "Development of Simulation Software Visualizing Seismic Wave Data to Extend Imagination for Building Response," Institute of Social Safety Science, No.17, pp. 129-134, 2012 (in Japanese).

Academic Societies & Scientific Organizations:
• Architectural Institute of Japan (AIJ)
• Japan Society for Disaster Information Studies (JSDIS)